ELSEVIER

Contents lists available at ScienceDirect

## Biosensors and Bioelectronics

journal homepage: www.elsevier.com/locate/bios





# A portable system for isothermal amplification and detection of exosomal microRNAs

Jingjing Qian<sup>a</sup>, Qinming Zhang<sup>a</sup>, Mingdian Liu<sup>a</sup>, Yixuan Wang<sup>a</sup>, Meng Lu<sup>a,b,\*</sup>

- a Department of Electrical and Computer Engineering, Iowa State University, Ames. IA, 50011, USA
- <sup>b</sup> Department of Mechanical Engineering, Iowa State University, Ames, IA, 50011, USA

#### ARTICLE INFO

Keywords: microRNA Exosome Exosomal microRNA isothermal PCR IoT

## ABSTRACTS

Exosomal microRNAs (miRNAs) play a key role in cell-cell communication to regulate gene expression in target cells and have great potential as biomarkers for disease diagnosis. This paper reports an on-chip exosomal miRNA amplification and detection system for rapid analysis of exosomal miRNAs. The compact system consists of two connected flow cells for processing exosomes and detecting miRNAs, respectively. The miRNAs extracted from exosomes were quantitatively measured using the on-chip exponential amplification reaction (EXPAR) assay. The sensor chip was designed to store multiple oligonucleotide templates for the EXPAR, mix sample and reagent, and simultaneously analyze multiple exosomal miRNAs of interest. To facilitate the miRNA analysis, a portable detection instrument was built on an IoT platform using a low-cost microcontroller to execute the EXPAR assay, collect fluorescent images, and analyze amplification curves. Here, we studied the miRNA profiles carried by exosomes derived from three different phenotypes of tissue macrophages. The affordable instrument, rapid assay, multiplexed analysis, as well as disposable sensor chip, would boost the development of point-of-care liquid biopsy tests using exosomal miRNAs.

## 1. Introduction

Short non-coding RNAs, which are known as microRNAs (miRNAs), participate in many fundamental cellular processes by post-transcription regulations (Bartel, 2004). Recent studies suggest that abnormal miRNA expression levels are closely related to many diseases, including cancers (Lujambio and Lowe, 2012). It has been shown that miRNAs function in several tumor-associated cell behaviors (Mitchell et al., 2008). In addition, since the miRNAs are cell-type-specific, the profile of miRNAs can be used to identify their parent cells. Therefore, the miRNAs circulating in body fluids have become promising biomarkers for liquid biopsy (Raser and O'Shea, 2004). There have been tremendous interests in the development of miRNA analysis assays for clinical diagnosis. In contrast to the circulating miRNAs, exosomal miRNAs are sorted and transported inside exosomes (EVs), which are 30-150 nm-diameter particles released from most cell types into the extracellular body fluids. Various exosomal nucleic acids, including mRNAs, miRNAs, and other non-coding RNAs, have recently been identified in the EVs (Valenciaet al., 2021). The exosomal miRNAs play key roles in cell-to-cell communication. Packed inside EVs, the exosomal miRNAs are highly stable and thus are considered as more reliable biomarkers to detect and monitor diseases (Sun Shiet al., 2018).

The rising applications of miRNA-based biomarkers demand for more rapid, sensitive, specific, and low-cost miRNA detection technologies (Laiet al., 2019; Xueet al., 2019; Ouyanget al., 2019). However, owing to miRNAs' short sequence lengths, high sequence similarity within families of expressed miRNAs, and large concentration range in parent cells, rapid analysis of miRNA targets is still challenging. The conventional quantitative PCR (qPCR) is not applicable to directly detecting miRNAs because the PCR primers for the short sequences are prone to generate primer dimers and the amplification lacks specificity. To address this problem, modified qPCR approaches, such as stem-loop reverse transcription (RT)-PCR, and polyadenylation of RNAs were developed (Chenget al., 2011; Foreroet al., 2019). Several hybridization-based sensors, such as electrochemical, optical, and transistor sensors, have also been demonstrated for miRNA detection without amplification (Gao Gaoet al., 2020; Frascella et al., 2015; El AamriMaliana Yammouriet al., 2020). On the other hand, miRNA profiling technologies, including the miRNA sequencing and microarray technologies, have been adopted for multiplexed miRNA analysis (Seashols-Williams Lewiset al., 2016; Ye Xuet al., 2019). Recently, isothermal amplification has emerged as a powerful method for the

<sup>\*</sup> Corresponding author. Department of Electrical and Computer Engineering, Iowa State University, Ames, IA 50011, USA. *E-mail address:* menglu@iastate.edu (M. Lu).

rapid detection of miRNAs (Deng et al., 2017). Isothermal amplification methods include rolling circle amplification, exponential amplification reaction (EXPAR), catalytic hairpin assembly, loop-mediated isothermal amplification, strand-displacement amplification, and hybridization chain reaction (Chenget al., 2009; Jiaet al., 2010; Daiet al., 2018; Sunet al., 2017; Shiet al., 2014; Geet al., 2014). The isothermal amplification provides appealing features of simple assay protocol, short assay time, high flexibility for multiplex miRNA targets, which are highly desired to develop point-of-care (POC) miRNA sensing technologies.

This work introduces a POC sensor system for rapid enrichment of EVs and detection of exosomal miRNAs, as shown in Fig. 1. The flow cell consists of two separated chips: the EV processing chip for EV enrichment and lysis (Fig. 1(a)), and the miRNA detection chip (Fig. 1(b)) to perform the multiplexed EXPAR analysis (Fig. 1(f)). These chips were connected using a plastic tube that was controlled by a solenoid pinch valve. The solenoid valve can shut off the sample flow between two chips by pinching the plastic tube. When the EVs were fully lysed, the sample flow was turned on to transfer the sample into the miRNA detection chip. As shown in Fig. 1(d) and (e), the EV extraction chip uses magnetic microbeads to extract the EVs from cell culture or body fluidic samples and subsequently lyse the EVs to release their miRNAs. Since the sample has been cleaned during the EV extraction step, it is possible to measure the released miRNAs without an RNA purification process to remove potential interfering molecules from complex samples. Here, the exosomal miRNAs are directly transferred into the miRNA detection chip to quantitatively measure the profile of miRNAs carried by the specific EV. The miRNA detection chip can measure up to eight different miRNAs using the on-chip EXPAR assay and a low-cost IoT reader. As an example, the exosomal miRNAs from three different macrophage phenotypes were investigated. The on-chip technology enables the analysis of exosomal miRNA in less than one and half hours.

#### 2. Experiments and methods

## 2.1. Materials and reagents

Diethylpyrocarbonate (DEPC)-treated water was obtained from Fisher Scientific Co. LLC. (Waltham, USA). All oligonucleotides were purchased from Integrated DNA Technologies (Coralville, USA). The WarmStart LAMP Master Mix (E1700L), SYBR-green fluorescence dye (B1700S), NEBuffer<sup>TM</sup> 3.1 (B7203S), and Nt.BstNBI nicking

endonuclease (R0607L) were purchased from New England Biolabs Inc. (Ipswich, USA). Single strand binding (SSB) protein was purchased from Sigma Aldrich Inc (St. Louis, USA). All solutions for EXPAR tests were prepared in the DEPC-treated water. The disposable sensor chips were made of 3-mm-thick acrylic sheet and patterned by a laser cutter. The microcontroller (ESP32, Espressif Systems) and CMOS camera (OV2640, OmniVision Technologies) were purchased from Digi-Key Electronics. The LED control board was custom-made with an array of 12 blue LEDs (732-4966-1-ND) and a LED driver (HV9803BLG-GCT-ND, Digi-Key Electronics). The excitation (FGB25) and emission filters (FGL530) were obtained from Thorlabs Inc.

## 2.2. Preparation, extraction, and lysis of EVs

EVs used in this study were secreted by murine macrophage cells (J774.1 cell line, ATCC). Murine macrophages were cultured in Dulbecco's Modified Eagle Medium (DMEM) containing 10% fetal bovine serum (Sigma-Aldrich) at 37 °C with 5% CO<sub>2</sub>. The culture medium with 10% fetal bovine serum (FBS) was filtered to remove EVs and stored at 4 °C before use. To produce polarized macrophages, the murine macrophages were chemically activated during cell culture. The M1 and M2 macrophages were activated by adding 100 ng/mL LPS (Sigma-Aldrich) and 20 ng/mL IL-4 (BioLegend, Inc.) in the culture media, respectively. After being cultured, we aspirated the medium to remove the dead cells and washed the flask with 10 mL DPBS (Dulbecco's Phosphate Buffered Saline, Thermo Fisher Scientific). Then, the cells were detached using a cell scraper and the solution was centrifuged at 1000 rpm min<sup>-1</sup> for 5 min. After aspirating the DPBS supernatant, the cell pellet was resuspended in a 600-µL culture medium and a 100-µL cell suspension was transferred to a new flask with 10-mL DMEM for cell culture. Usually, the macrophages can reach to  $\sim$ 90% confluency on day three of subculturing. The EVs were sampled from naïve, M1, and M2 macrophage cultures when cells reached 90% confluency. Before pumping EV samples into the flow cell, the samples were filtered using 0.22-µm filters to remove the cells and debris.

The  $3-\mu m$ -diameter microbeads (MC3000, Ocean NanoTech) were carboxyl acid-modified and functionalized using CD63 antibody (antimouse CD63 antibody, BioLegend). Before coating the CD63 antibody, the microbeads were activated using an EDC/sulfo-NHS covalent coupling procedure by mixing the microbeads (10 mg/mL), 0.2 mL activation buffer, and 20- $\mu$ L EDC solution (20 mg/mL) for 15 min at

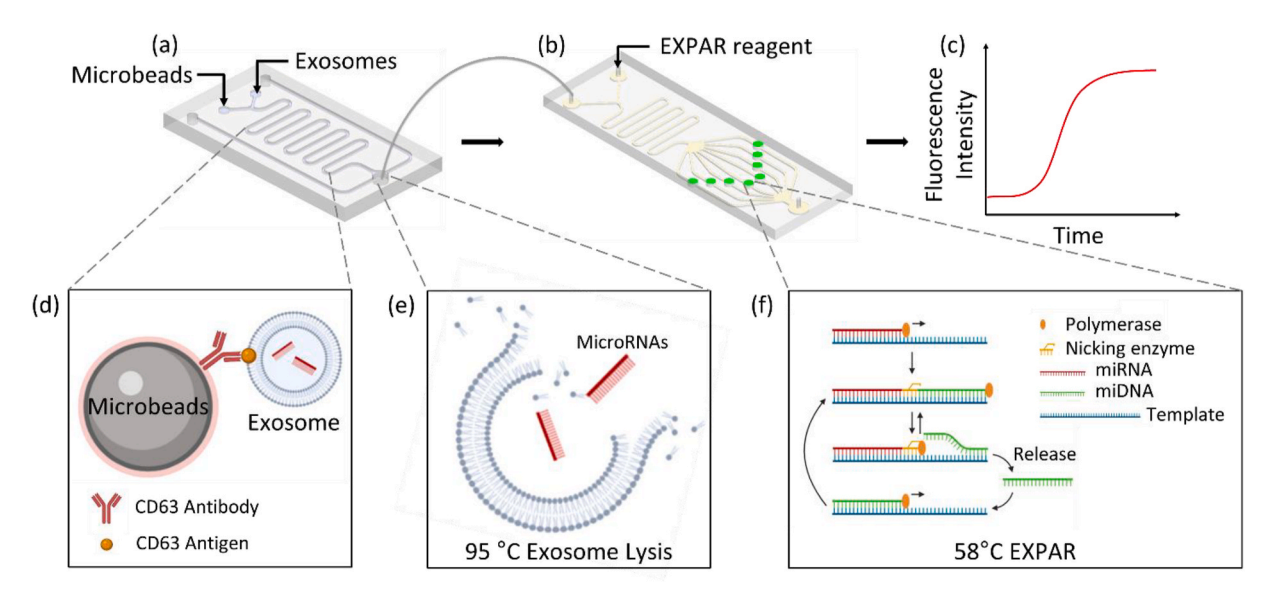


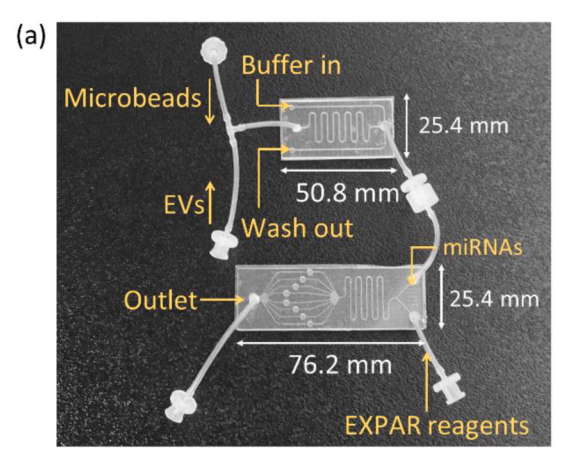
Fig. 1. Schematic diagram of the on-chip exosomal miRNA analysis assay. (a)–(c) Schematic diagrams of the EV extraction and lysis chip, miRNA detection chip, and EXPAR amplification curve, respectively. (d) Conjugation of anti-CD63 antibody-coated magnetic beads to an EV via its surface CD63 antigens. (e) EV lysis at 95 °C to release exosomal miRNAs. (f) Isothermal EXPAR assay to amplify and detect miRNA using a specific oligonucleotide template.

room temperature. Then, the CD63 antibody (1 mg/mL) was added into the microbeads solution, and the mixture was incubated for 2.5 h at room temperature. After the CD63 antibody conjugation, the surface of the microbeads was blocked using a quenching buffer (Ocean Nano-Tech) for 30 min. To collect the CD63-coated microbeads, the mixture was placed on a magnetic separator for 20 min, the supernatant was removed, and the microbeads were resuspended in phosphate-buffered saline (PBS) solution (Niuet al., 2020). The microbeads were washed three times, and the resuspended microbeads were stored in PBS at 4 °C for future use.

The chip for exosome extraction and lysis has three 3-mm-diameter inlets, a 145-mm-long on-chip mixer, a 5-mm-diameter extraction chamber, and two 3-mm-diameter outlets, as shown by the top chip in Fig. 2(a). The width of all channels is 0.2 mm. During the incubation step, the CD63 antibody-coated microbeads and CD63 antigen-coated exosome samples are pumped into the mixer at the flow rate of 0.3 μL/min. The EVs bind to the magnetic microbeads in the mixing channel. Then, the EV-conjugated microbeads are collected in the extraction chamber by a permanent magnet placed right below the chamber. Fig. 2 (b) shows the SEM image of the EVs attached to the microbeads. The EVmicrobead mixture continuously flows through the extraction chamber and exits the chip from the waste outlet. To characterize the EV enrichment efficiency, the initial EV sample and the sample collected from the waste outlet were measured using a nanoparticle tracking tool (NS300 NanoSight) (Zhanget al., 2021). The change of nanoparticle count was calculated for the particles' diameter from 80 to 120 nm to estimate the EV capture efficiency of approximately 50%. The total sample volume flowed through the extraction chamber was 3 mL with the EV concentrations of  $3 \times 10^6$  particles/mL. With the permanent magnet in place, the extraction chamber was washed to remove interfering molecules. The collected EV-microbead conjugates were resuspended in a 14  $\mu L$  DEPC-treated water before lysing the EVs. The purified EV concentration was approximately  $6.42 \times 10^8$  EV/mL, which represented an enrichment factor over 200 times. Then, EVs were lysed by heating the chamber at 95 °C for 10 min. The EV lysis was subsequently pumped into the miRNA detection chip without a nucleic acid purification process. The magnetic beads-based EV extraction enables the detection of exosomal miRNAs in complex samples by boosting the EV concentration and removing interfering molecules, such as DNA, RNA, and proteins.

## 2.3. On-chip exponential isothermal amplification (EXPAR) of miRNAs

The miRNA detection chip consists of two inlets, one mixture, eight 2-mm-diameter reaction chambers, and one outlet (bottom chip in Fig. 2



(a)). The depth of the reaction chambers is 1.5 mm to hold an approximately 4.7-µL mixture of EXPAR reagent and lysed exosome. The EXPAR reagent consisted of SSB protein (2 µM), RNase inhibitor (0.8 U/ µL), SYBR-green dye (0.4 µg/mL), WarmStart Lamp Master Mix (1X), and nicking endonuclease (0.4U/µL) were dissolved in the buffer (NEBuffer 3.1, NEB). The single-stranded template DNAs (ssDNAs) were dissolved in the DEPC water at 25 nM, pipetted into the reaction chambers, and dried in the air before the chip was sealed. The miRNA and EXPAR reagent mixing ratio was approximately 1:9. Before starting an EXPAR amplification, the mixture filled the reaction chambers to wet the template ssDNAs. The EXPAR tests were performed at 58 °C for less than 1 h. The fluorescence images of the chambers were captured at intervals of 30 s during the process.

## 2.4. EXPAR amplification and template design

The principle of the EXPAR amplification is illustrated in Fig. 3(a) (Jiaet al., 2010). The ssDNA template contains two identical sequences at the 3' terminus and the 5' terminus, and a nicking endonuclease recognition sequence 3'-CTCAG-5' in the center. If the target miRNA is complementary to the template, it can hybridize with the template, then be extended along with the template by a strand-displacement polymerase (Bst 2.0 DNA polymerase) to form a double-stranded DNA (dsDNA). Then, the nicking endonuclease cleaves the dsDNA at the recognition site to break the replicated strand into two identical segments. The replicated ssDNA is released from the template by the Bst polymerase and participates in the amplification process together with the target miRNA molecules. Repeating this process would contribute to the exponential amplification of the target miRNA. The amount of dsDNA product can be measured using the dsDNA binding SYBR-green dye. To prevent non-specific bindings, the templates are protected by SSB protein (Reidet al., 2018). The sequences of the miRNAs, including the miR-223, miR-210, miR-146b, and miR-127, and their corresponding templates are given in Fig. 3(b).

## 2.5. Portable miRNA analyzer

To facilitate the real-time measurement of SYBR green emission during an EXPAR reaction, we designed a portable EXPAR detector (Fig. 3(a)), which was controlled using an ESP32 microcontroller (Liu et al., 2020). The compact system offers three main functions, including temperature management, fluorescence detection, and data transmission to cloud storage. The fluorescence detector, consisting of the blue LED array (P=360 mW), CMOS camera, and optical filters, was built to measure the SYBR-green emission from the EXPAR chip (Fig. 3

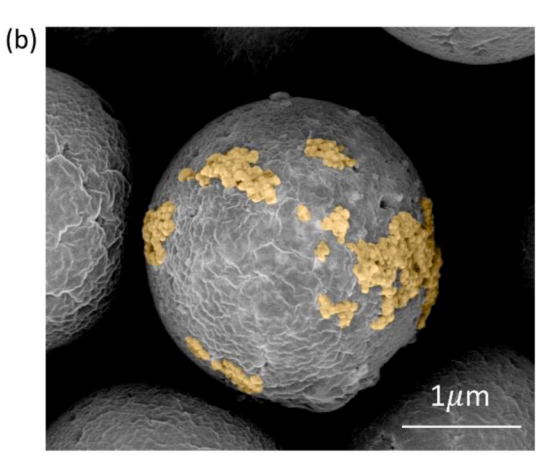


**Fig. 2.** Flow cell for the analysis of exosomal miRNAs. (a) Photograph of the assembled exosome lysis chip and miRNA detection chip. The depths of the flow channel and reaction chambers are 0.5 mm and 1.5 mm, respectively. (b) Scanning electron microscopy (SEM) image of the exosomes captured on magnetic beads. The EVs are highlighted in yellow. (For interpretation of the references to colour in this figure legend, the reader is referred to the Web version of this article.)

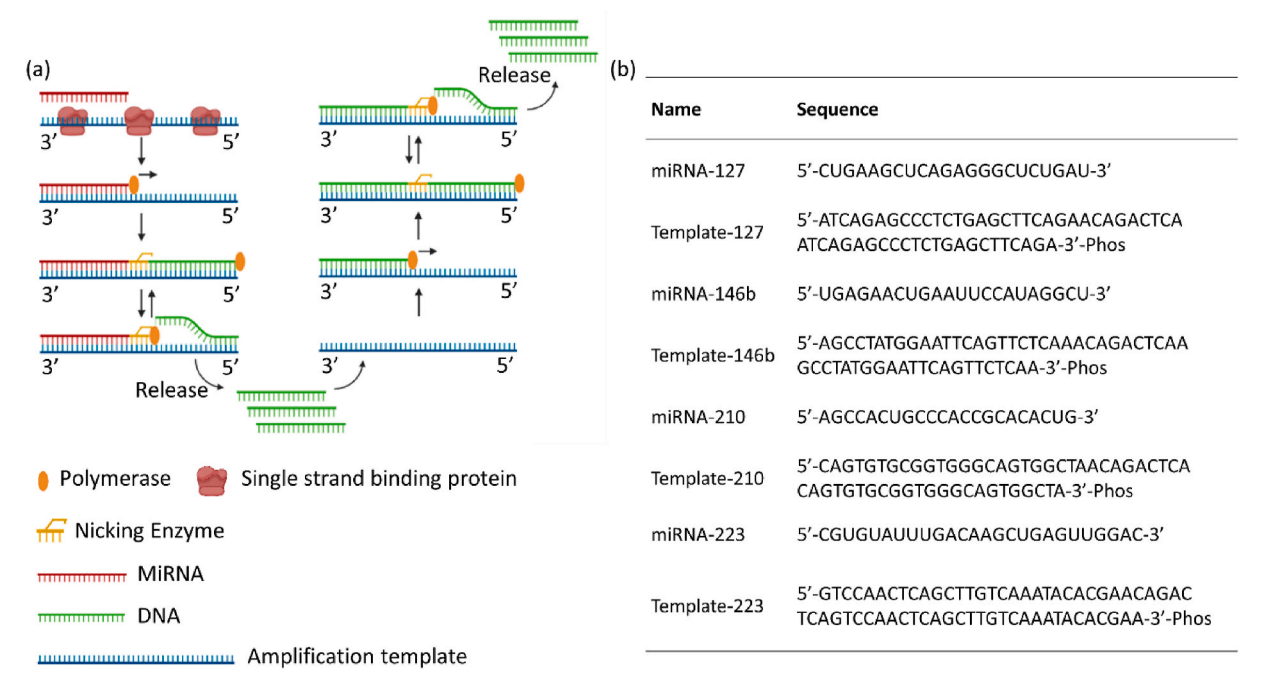


Fig. 3. Design of the EXPAR assay. (a) Schematic representation of the EXPAR assay that amplifies the target miRNA using the specific template, strand-displacement polymerase, and nicking enzyme. The amount of EXPAR product can be quantified using a dsDNA binding dye, such as SYBR-green. (b) Sequences of four target miRNAs used in this work and the corresponding amplification templates. The 3′ end of these templates is terminated by a phosphate group (-Phos). (For interpretation of the references to colour in this figure legend, the reader is referred to the Web version of this article.)

(b)). The ESP32 microcontroller can turn on/off the LEDs, acquire images from the CMOS camera, and transfer the images to the cloud data storage via a WiFi network. These images were processed using a Google Apps Script to generate the amplification curve for each reaction chamber. The ESP32 microcontroller was connected to a thermocouple (K-type, Omega Engineering) and the switch of a thermoelectric cooler (TEC). During EXPAR experiments, the temperature was maintained at 58 °C, and fluorescence images (such as Fig. 4(a)) were captured every minute and transmitted to the Google Drive folder. The housing for the fluorescence image and temperature was built using a 3D printer to block unwanted ambient light.

#### 3. Results and discussion

#### 3.1. Quantitative EXPAR detection of microRNA on chip

For a quantitative EXPAR assay, the time to the threshold ( $T_t$ ) is usually used to determine the miRNA concentration. Here we define the

time when the fluorescence intensity reaches 20% of the maximum fluorescence value as the  $T_t$ . To calculate the  $T_t$  value, the amplicons produced by an EXPAR reaction were measured in real-time using the fluorescence detector. The miRNA-223 was chosen to demonstrate the process. A ten-fold miRNA-223 dilution serial was prepared with the miRNA concentration ranging from 100 nM to 100 fM using DEPCtreated water. The diluted samples were pipetted and stored in the reaction chambers along with an empty chamber, which served as the negative control. After sealing the flow cell, the EXPAR reagent and ssDNA template was injected into the chip. Fluorescence images were measured every 30-sec unit all fluorescence intensities from all reaction chambers stabilized. Fig. 5(a) compares the fluorescence images collected during the amplification of miRNA-223 at 15 min, 20 min, 25 min, and 30 min, respectively. The increase of the fluorescence emission from the reaction chambers corresponds to the production of dsDNA amplicons. The average fluorescence intensity at each reaction chamber was calculated and plotted as a function of time as the amplification curves shown in Fig. 5(b).

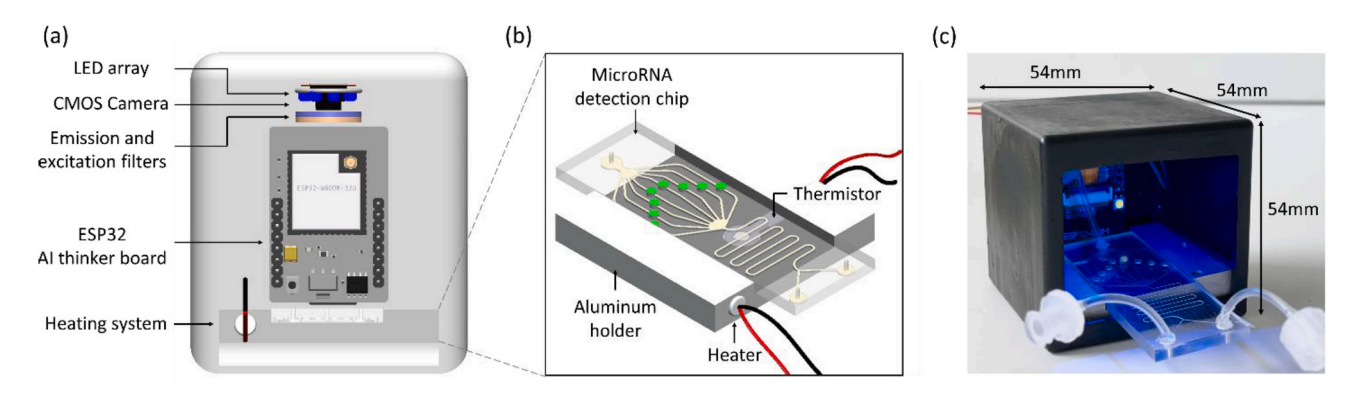
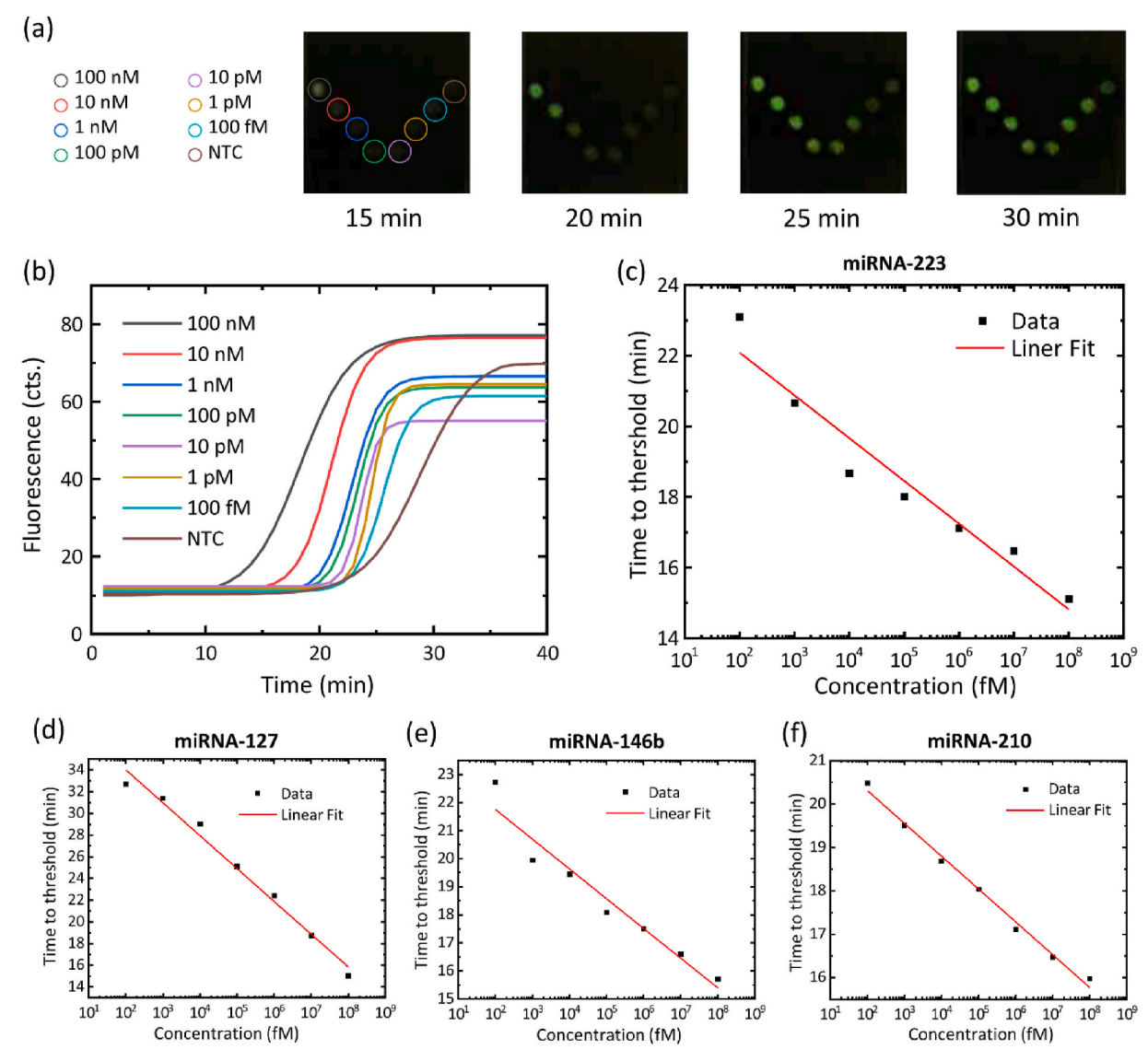


Fig. 4. IoT-based EXPAR instrument. (a) Design of the POT miRNA analysis system with the dimension of  $54 \text{ mm} \times 54 \text{ mm} \times 54 \text{ mm} \times 64 \text{ mm}$ 



**Fig. 5.** On-chip quantitative analysis of miRNAs. (a) Fluorescent images of the miRNA detection chip during an EXPAR test for a dilution serial of miRNA-223. The fluorescence images were captured at 15, 20, 25, and 30 min, respectively. (b) Amplification curves generated for the miRNA-223 test with the miRNA-223 concentration ranging from 100 fM to 100 nM. (c) Calculated  $T_t$  values vs. miRNA-233 concentration. (d)–(f)  $T_t$  values vs. miRNA concentration for miRNA-127, miRNA-146b, and miRNA-210, respectively.

The T<sub>t</sub> values were calculated and plotted versus the miRNA-223 concentration in Fig. 5(c). The  $T_t$  values were approximately 15 min and 22 min for the 100 nM and 100 fM samples, respectively. It can be seen from the linear fitting that the  $T_t$  value decreased proportionally with the increase of the miRNA concentration. The result of this realtime EXPAR data collection and  $T_t$  value analysis suggested that the sensor system is fully quantitative. Next, we prepared and tested ten-fold dilution serials for miRNA-127, miRNA-146b, and miRNA-210 with the miRNA concentration from 100 nM to 100 fM. Fig. 5(d)–(f) show the  $T_t$ response curve for miRNA-127, miRNA-146b, and miRNA-210, respectively. These dose response curves were used as the calculation data for the study of exosomal miRNA profiles in macrophage-derived EVs. Previous study reported that on average, each EV particle could contain approximately 0.1-100 copies of these four miRNAs (Zhang et al., 2013; Paolaet al., 2019; Leeet al., 2013; Lanet al., 2020). Assuming the magnetic beads purified EV has the concentration of  $6.42 \times 10^8$  EV/mL, the miRNA concentration is in the range of  $10^2-10^5$  fM, which falls in the sensitivity range of the on-chip EXPAR assay.

## 3.2. Simultaneous detection of multiple miRNAs in exosomes

To use exosomal miRNAs as diagnostic biomarkers, it is necessary to identify the change of miRNA profile by simultaneously measuring the concentrations of multiplex miRNAs in the carrier EVs (Bhomeet al., 2018). Here, four exosomal miRNAs, including miRNA-127, miR-NA-146b, miRNA-210, and miRNA-223, were chosen to demonstrate the multiplexed on-chip EXPAR assay. Prior studies have shown that these miRNAs play important roles in macrophage polarization and were also found in macrophage-derived EVs (Yinget al., 2015; Chouet al., 2017; Zenget al., 2011; Gaoet al., 2017; Johnnidis et al., 2008). It has also been demonstrated that the EXPAR assay's specificity can be significantly high to distinguish miRNAs with highly similar sequences (Jiaet al., 2010). The high specificity allows us to simultaneously detect multiple miRNAs from EV lysates.

In this test, the templates corresponding to these miRNAs were designed and stored in the specific reaction chambers. Two reaction chambers were used for each miRNA. The lysed EV sample and EXPAR reaction reagent were pumped into the inlets of the miRNA detection chip and mixed by the mixer channel. When all eight reaction chambers

were fully filled, the EXPAR process started by setting the chip temperature at 58 °C and recording fluorescence images every 30 s. The amplification curves of these miRNAs are compared in Fig. 6(a). Then the T<sub>t</sub> values were found for the miRNA-127, miRNA-146b, miRNA-210, and miRNA-223, respectively. Referenced to the calibration curves shown in Fig. 5(c)-(f), the concentrations of each miRNA could be calculated by substitute the  $T_t$  value into the linear fit function of each miRNA. The concentration of the miRNA-127, miRNA-146b, miRNA-210, and miRNA-223 in  $\ensuremath{\text{EV}_{\text{M0}}}$  are compared in Fig. 6(b). The miRNA-146b exhibited the highest concentration and miRNA-210 showed the lowest concentration, which agreed with the miRNA profile of naïve macrophage (Italiani and Boraschi, 2014). The specificity of the EXPAR assay was studied by the amplification of miRNA-210 in the presence of the other three miRNAs. Three EXPAR reactions of mixing all four miRNAs (miRNA-210, -146b, -223, -127) with the miRNA-210 template, three miRNAs (miRNA-146b, -223, -127) with the miRNA-210 template, and all miRNAs without any template, were performed, respectively. For the sample contained both miRNA-210 and its template, the  $T_t$  value was 18 min. In contrast, the samples without miRNA-210 or the miRNA-210 template had much longer  $T_t$  values of 28 min and 31 min, respectively.

## 3.3. Profiling of miRNAs in EVs derived by macrophage phenotypes

As an in-vitro diagnosis approach, the EV analysis should provide sufficient information to identify EV's parental cells and their physiological changes. Owning to the remarkable plasticity, macrophages can undergo specific differentiation and differentiate into phenotypes with distinct functions in local tissue environments (Mendoza-Coronel et al., 2016). Activated by external stimuli, the naïve macrophages (MO) can

express phenotypes ranging from M1 to M2 macrophages in pro-inflammatory and T<sub>H</sub>2 immune response environments, respectively (Wang Zhanget al., 2021; Wanget al., 2018). It has been demonstrated that some miRNA contents vary significantly in M0, M1, and M2 macrophages (Essandohet al., 2016). Many studies have used microarray and RT-qPCR array technology to determine the miRNA expression profile in M1 and M2 polarized human and murine macrophages (Seashols-Williams Lewiset al., 2016). More specifically, miRNA-127 showed a higher concentration in M1 polarized macrophage compared to naïve and M2 macrophages. The miRNA-210 and miRNA-223 shown higher concentration in M2 polarized macrophage, and miRNA-146b shown higher concentration in naïve macrophages (Mendoza-Coronel et al., 2016; Essandohet al., 2016; Zhanget al., 2013). Our hypothesis is that the changes of these miRNA concentrations should also be reflected in the macrophage-derived EVs. Here, we used three chips to analyze the miRNA-127, miRNA-146b, miRNA-210, and miRNA-223 in EVs secreted from three macrophage phenotypes. The naïve macrophage was activated using LPS and IL-4 to produce M1 and M2 EVs, as shown in Fig. 6 (c). Details of the macrophage polarization process have been reported in our previous works (Zhanget al., 2021; Italiani and Boraschi, 2014). The EVs were collected and enriched using the magnetic microbeads and subsequently lysed to extract miRNAs. The miRNAs were mixed with the EXPAR reagents and measured in the reaction chambers to find the  $T_t$ values. The concentration of each miRNA was calculated using the dose-response curve for the specific type of miRNA in Fig. 5(c)-(f). The miRNAs concentrations for EV<sub>M0</sub>, EV<sub>M1</sub>, and EV<sub>M2</sub> were compared in Fig. 6(d). Consistent with previous research results, miRNA-210 and miRNA-223 showed higher concentration in EV<sub>M2</sub>, miRNA-146b showed the highest concentration in EV<sub>M0</sub>, miRNA-127 had the highest concentration in EV<sub>M1</sub> (Essandohet al., 2016). In addition to the

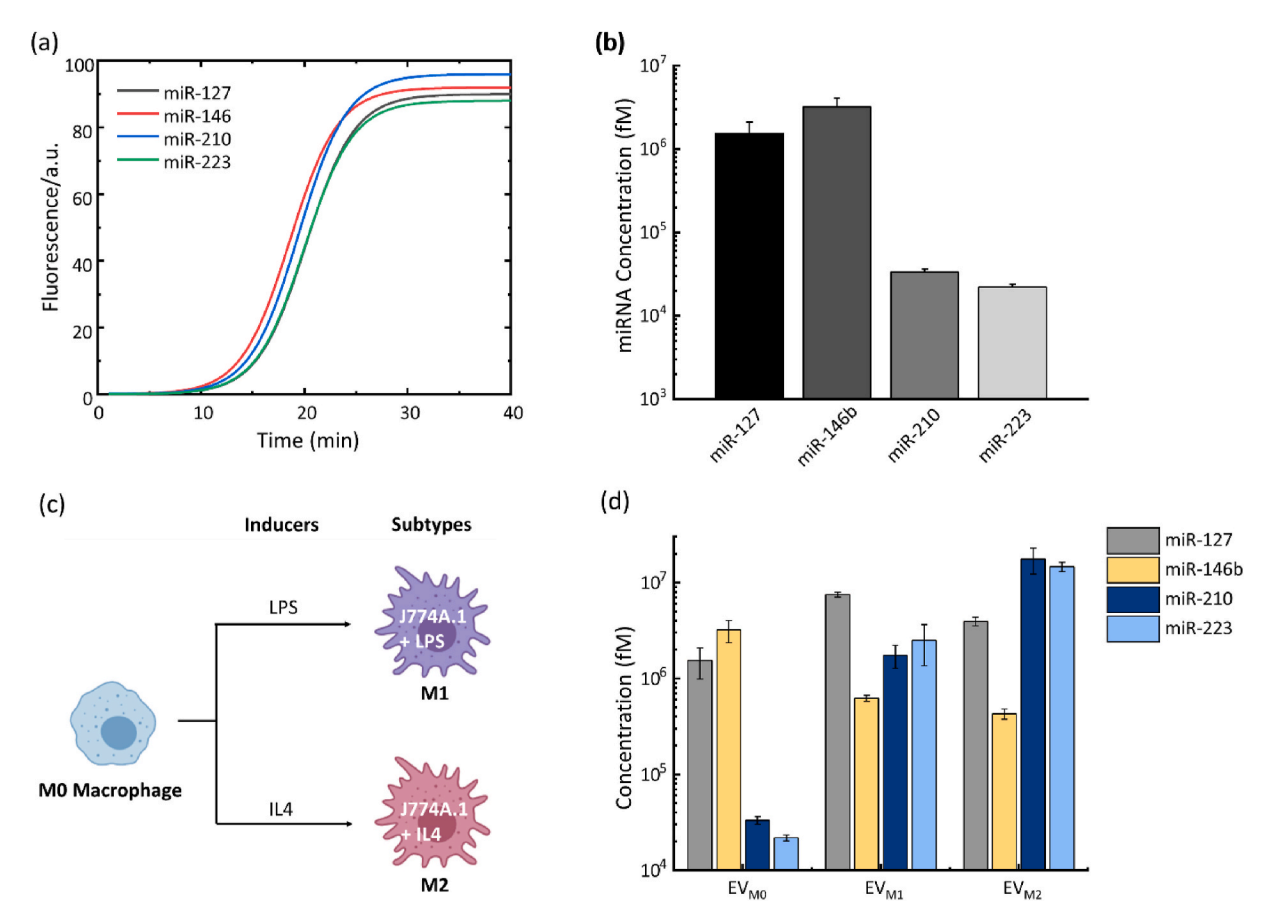


Fig. 6. Simultaneous detection of multiple miRNAs contents in EVs derived from three macrophage phenotypes. (a) Amplification curves for four different miRNAs from the  $EV_{M0}$ . (b) The calculated concentration of each miRNA carried by the  $EV_{M0}$ . (c) Schematics of macrophage polarization from M0 to M1 and M2 macrophages. (d) Calculated miRNA concentrations for EVs derived from M0, M1, and M2 macrophages.

polarization of macrophages, the expression levels of miRNA-223, miRNA-146b, and miRNA-210 have been used as human disease biomarkers (Paolaet al., 2019; Leeet al., 2013; Lanet al., 2020).

#### 4. Conclusion and discussion

This work demonstrated an on-chip miRNA analysis technology that can characterize a panel of exosomal miRNAs to distinguish EVs derived from similar originating cells. The exosomal miRNA analysis consists of two connected flow cells for the enrichment of EVs and detection of EV-released miRNAs, respectively. The miRNA detection is based on the isothermal EXPAR amplification using ssDNA templates pre-stored in the on-chip reaction chambers. The advantages of the rapid exosomal miRNA assay include the multiplexed detection, low-cost and disposable sensor, short detection time of 30 min, and no need of RNA extraction for complex samples. The results showed that we could use the analysis of four miRNAs to identify EVs released by macrophages and discriminate between EVs from polarized and non-polarized parental macrophages. The combination of these miRNAs provides a panel of biomarkers to detect the physiological changes to the parent cells of EV.

The exosomal miRNA sensor technology can be further improved from the following aspects. First, the flow cell with a higher density of reaction chambers will be implemented to study a larger panel of miR-NAs. The diagnosis of complex diseases, such as cancers, usually requires the detection of a large number of aberrant miRNAs (Bhome et al., 2018; Thind and Wilson, 2016). The measurement of full miRNA expression profiles with a lower cost and shorter assay time than the sequencing method is highly desired for diagnostic applications. Using microfluidics with higher precision and better control of liquid flow will help to automate the developed exosomal miRNA detection assay. Second, to simplify the assay, the EXPAR regents can be lyophilized inside the flow cell. The on-chip storage capability will eliminate the need for preparing and injecting the reagents by users. Third, the data analysis functions can be integrated into the ESP32 microcontroller to plot the amplification curves and calculate miRNA concentrations in situ. A fully integrated exosomal miRNA analyzer will benefit EV-based disease diagnostics and therapeutics.

## CRediT authorship contribution statement

Jingjing Qian: Conceptualization, Investigation, Methodology, Validation, Writing – original draft, Writing – review & editing. Qinming Zhang: Investigation, Resources, Methodology. Mingdian Liu: Methodology, Resources. Yixuan Wang: Software. Meng Lu: Conceptualization, Methodology, Writing – original draft, Writing – review & editing.

## Declaration of competing interest

The authors declare that they have no known competing financial interests or personal relationships that could have appeared to influence the work reported in this paper.

## Acknowledgments

This research was supported by the National Science Foundation under grant ECCS 16-53673, and the National Institute of Food and Agriculture under Award No. 2018-67021-27968. Any opinions, findings, and conclusions or recommendations expressed in this material are those of the author(s) and do not necessarily reflect the views of the National Science Foundation. The authors would thank Prof. Michael Kimber and Mr. Leland Harker of Iowa State University for providing the macrophages and fabricating the acrylic chips, respectively.

#### References

- Bartel, D.P., 2004. MicroRNAs: genomics, biogenesis, mechanism, and function. Cell 116, 281–297
- Bhome, Rahul, Del Vecchio, Filippo, Lee, Gui-Han, Bullock, Marc D., John, N., Primrose, A., 2018. Emre Sayan, and Alex H. Mirnezami. "Exosomal microRNAs (exomiRs): small molecules with a big role in cancer. Cancer Lett. 420, 228–235.
- Bhome, Rahul, et al., 2018. Exosomal microRNAs (exomiRs): small molecules with a big role in cancer. Cancer Lett. 420, 228–235.
- Cheng, Yongqiang, et al., 2009. Highly sensitive determination of microRNA using target-primed and branched rolling-circle amplification. Angew. Chem. 48, 3268–3272.
- Cheng, Caifu, et al., 2011. Quantitation of microRNAs by real-time RT-qPCR. Methods Mol. Biol. 687, 113–134.
- Chou, Chen-Kai, et al., 2017. MicroRNA-146b: a novel biomarker and therapeutic target for human papillary thyroid cancer. Int. J. Mol. Sci. 18, 636.
- Dai, Wenhao, et al., 2018. Catalytic hairpin assembly gel assay for multiple and sensitive microRNA detection. Theranostics 8 (10), 2646–2656.
- Deng, Ruijie, Zhang, Kaixiang, Li, Jinghong, 2017. Isothermal amplification for MicroRNA detection: from the test tube to the cell. Acc. Chem. Res. 50, 1059–1068.
- El Aamri, Maliana, Yammouri, Ghita, et al., 2020. Biosensors for detection of MicroRNA as a cancer biomarker: pros and cons. Biosensors 11, 186.
- Essandoh, Kobina, et al., 2016. MiRNA-mediated macrophage polarization and its potential role in the regulation of inflammatory response. Shock 46, 122–131.
- Forero, Diego A., et al., 2019. qPCR-based methods for expression analysis of miRNAs. Biotechniques 67 (4).
- Frascella, F., Ricciardi, S., et al., 2015. Enhanced fluorescence detection of miRNA-16 on a photonic crystal. Analyst 140, 5459–5463.
- Gao, Jianwei, Gao, Yakun, et al., 2020. Ultrasensitive label-free MiRNA sensing based on a flexible graphene field-effect transistor without functionalization. ACS Applied Electronic Materials 4, 1090–1098.
- Gao, Yunliang, et al., 2017. The role of miRNA-223 in cancer: function, diagnosis and therapy. Gene 616, 1–7.
- Ge, Zhilei, et al., 2014. Hybridization chain reaction amplification of MicroRNA detection with a tetrahedral DNA nanostructure-based electrochemical biosensor. Anal. Chem. 86, 2124–2130.
- Italiani, Paola, Boraschi, Diana, 2014. From monocytes to M1/M2 macrophages phenotypical vs. Functional differentiation. Front. Immunol. 5, 514.
- Jia, Hongxia, et al., 2010. Ultrasensitive detection of microRNAs by exponential isothermal amplification. Angew. Chem. Int. Ed. 49, 5498–5501.
- Johnnidis, J.B., et al., 2008. Regulation of progenitor cell proliferation and granulocyte function by microRNA-223. Nature 451, 1125–1129.
- Lai, Meimei, et al., 2019. Label-Free MicroRNA optical biosensors. Nanomaterials 9 (11), 1573.
- Lan, Fengming, et al., 2020. Exosomal microRNA-210 is a potentially non-invasive biomarker for the diagnosis and prognosis of glioma. Oncol Lett 19 (3), 1967–1974.
- Lee, James C., et al., 2013. MicroRNA-222 and MicroRNA-146b are tissue and circulating biomarkers of recurrent papillary thyroid cancer. Cancer 119, 4358–4365.
- Liu, Mingdian, Monshat, Hosein, Tang, Zheyuan, Wu, Zuowei, Zhang, Qijing, Lu, Meng, 2020. An IoT-enabled paper sensor platform for real-time analysis of isothermal nucleic acid amplification tests. Biosens. Bioelectron. 169, 12651 https://doi.org/10.1016/j.bios.2020.112651.
- Lujambio, A., Lowe, S.W., 2012. The microcosmos of cancer. Nature 482, 347–355.
  Mendoza-Coronel, Elizabeth, et al., 2016. Infection of J774A.1 with different
  Mycobacterium species induces differential immune and miRNA-related responses.
  Microbiol. Immunol. 60, 356–363.
- Mitchell, P.S., Parkin, R.K., et al., 2008. Circulating microRNAs as stable blood-based markers for cancer detection. Proc. Natl. Acad. Sci. U. S. A 105, 10513–10518.
- Niu, Fuzhou, et al., 2020. Integrated immunomagnetic bead-based microfluidic chip for exosomes isolation. Micromachines 11 (5), 503.
- Ouyang, Tinglan, et al., 2019. MicroRNA detection specificity: recent advances and future perspective. Anal. Chem. 91 (5), 3179–3186.
- Paola, D'Antona, et al., 2019. Serum miR-223: a validated biomarker for detection of early-stage non-small cell lung cancer. Cancer Epidemiology and Prevention Biomarkers 28 (11), 1926–1933.
- Raser, J.M., O'Shea, E.K., 2004. Control of stochasticity in eukaryotic gene expression. Science 304, 1811–1814.
- Reid, Michael S., et al., 2018. Reduction of background generated from templatetemplate hybridizations in the exponential amplification reaction. Anal. Chem. 90, 11033–11039.
- Seashols-Williams, S., Lewis, Carolyn, et al., 2016. High-throughput miRNA sequencing and identification of biomarkers for forensically relevant biological fluids. Electrophoresis 21, 2780–2788.
- Shi, Chao, et al., 2014. Exponential strand-displacement amplification for detection of MicroRNAs. Anal. Chem. 86, 336–339.
- Sun, Zhenqiang, Shi, Ke, et al., 2018. Effect of exosomal miRNA on cancer biology and clinical applications. Mol. Cancer 17, 147.
- Sun, Yuanyuan, et al., 2017. One-step detection of microRNA with high sensitivity and specificity via target-triggered loop-mediated isothermal amplification (TT-LAMP). Chem. Commun. 53 (80), 11040–11043.
- Thind, Arron, Wilson, Clive, 2016. Exosomal miRNAs as cancer biomarkers and therapeutic targets. J. Extracell. Vesicles 5 (1), 31292.
- Valencia, Karmele, et al., 2021. Exosomes in liquid biopsy: the nanometric world in the pursuit of precision oncology. Cancers 13 (9), 2147.

- Wang, Yifei, Zhang, Qinming, et al., 2021. Hyperspectral imaging-based exosome microarray for rapid molecular profiling of extracellular vesicles. Lab Chip 21, 196–204.
- Wang, Yifei, et al., 2018. Rapid differentiation of host and parasitic exosome vesicles using microfluidic photonic crystal biosensor. ACS Sens. 3 (9), 1616–1621.
- Xue, Tianyu, et al., 2019. Ultrasensitive detection of miRNA with an antimonene-based surface plasmon resonance sensor. Nat. Commun. 10, 28
- Ye, Jiawei, Xu, Mingcheng, et al., 2019. Research advances in the detection of miRNA. Journal of Pharmaceutical Analysis 9, 217–226.
- Ying, Hangjie, et al., 2015. MiR-127 modulates macrophage polarization and promotes lung inflammation and injury by activating the JNK pathway. J. Immunol. 194, 1230-1251
- Zeng, Lili, et al., 2011. MicroRNA-210 as a novel blood biomarker in acute cerebral ischemia. Frontiers in Bioscience-Elite 3, 1265–1272.
- Zhang, Yingying, et al., 2013. Expression profiles of miRNAs in polarized macrophages. Int. J. Mol. Med. 31 (4), 797-802.
- Zhang, Yingying, et al., 2013. Expression profiles of miRNAs in polarized macrophages. Int. J. Mol. Med. 31, 797–802.
- Zhang, Qinming, et al., 2021. Towards Nanovesicles-Based Disease Diagnostics: A Rapid Single-step Exosome Assay within One Hour through In-Situ Immunomagnetic Extraction and Nanophotonic Label-free Detection,". Lab chip.